LANGMUIR Article
Cite This: Langmuir 2017, 33, 12719-12728 pubs.acs.org/Langmuir

Aggregation of a Cationic Gemini Surfactant with a Chelating Molecule and Effects from Calcium Ions

Weiwei Zhao,[†,§,∥] Kai Song,[‡,§] Yao Chen,[†,§] Hua Wang,[†,§] Zhang Liu,[†,§] Qiang Shi,[‡,§] Jianbin Huang,[∥] and Yilin Wang*[,†,§]

[†]CAS Key Laboratory of Colloid, Interface and Chemical Thermodynamics and [‡]State Key Laboratory for Structural Chemistry of Unstable and Stable Species, Beijing National Laboratory for Molecular Sciences (BNLMS), CAS Research/Education Center for Excellence in Molecular Sciences, Institute of Chemistry, Chinese Academy of Sciences, Beijing 100190, P. R. China

[§]University of Chinese Academy of Sciences, Beijing 100049, P. R. China

[∥]Beijing National Laboratory for Molecular Sciences (BNLMS), College of Chemistry and Molecular Engineering, Peking University, Beijing 100871, P. R. China

Supporting Information

ABSTRACT: The aggregation behavior of cationic ammonium gemini surfactant hexamethylene-1,6-bis(dodecyldimethylammonium bromide) (12-6-12) with chelating molecule ethylenediaminetetraacetic acid (EDTA) and the effects of calcium bromide ($CaBr_2$) on the structure and morphology of the aggregates in the mixture have been investigated by surface tension, isothermal titration microcalorimetry, electrical conductivity, ζ potential, dynamic light scattering, cryogenic transmission electron microscopy, freeze−fracture transmission electron microscopy, and ^{1}H NMR techniques. It was found that the electrostatic attraction between the carboxyl groups of EDTA and the headgroups of 12-6-12 leads to the formation of oligomeric-like surfactant EDTA$(12\text{-}6\text{-}12)_2$ at an EDTA/12-6-12 molar ratio of 0.50. The critical aggregation concentration of the EDTA$(12\text{-}6\text{-}12)_2$ complexes is much lower than that of 12-6-12, and the complexes form loose, large network-like premicellar aggregates and then transfer into small micelles with an increase in concentration. Moreover, the addition of $CaBr_2$ induces the transition from the loose aggregates and micelles to vesicles owing to the coordination interaction between the calcium ion and EDTA and the electrostatic interaction between EDTA and 12-6-12. The work reveals that as a bridging molecule between the calcium ion and the gemini surfactant, the chelating molecule greatly promotes the assembly of the gemini surfactant and strengthens the molecular packing in the presence of calcium ions.

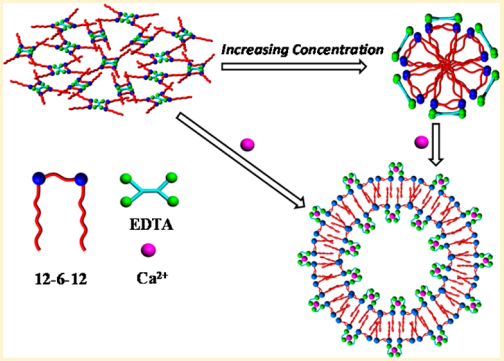

INTRODUCTION

The calcium ion is one of the main components in hard water and can induce a serious salting-out phenomenon in an aqueous solution of ionic surfactants.[1−4] It significantly elevates the Krafft points[5] of ionic surfactants and decreases the surfactant solubility in water.[6−11] The problem seriously limits the applications of surfactant household and industrial products in water of a high hardness level and weakens the cleaning efficiency of detergents. To solve this problem, chelating molecule ethylenediaminetetraacetic acid (EDTA) is often applied in detergents to prevent the precipitation of surfactants by forming strong, water-soluble metal complexes with transition-metal ions.[12] It has also been approved that EDTA cannot be absorbed into the skin or be bioaccumulated in living organisms.[13,14] Gemini surfactants possess two amphiphilic moieties connected by a spacer at the level of headgroups. Compared to conventional single-chain surfactants, gemini surfactants have lower critical micellization concentrations (CMCs), lower Krafft points, and diverse aggregation morphologies and other unique properties.[15−21] Ionic gemini surfactants may show a different binding situation with either EDTA or calcium ions from conventional single-chain surfactants. Therefore, understanding the effect of Ca^{2+} ions on the aggregation behavior of ionic gemini surfactants in the presence of EDTA will guide the applications of gemini surfactants in hard water.

Understanding the binding situation of EDTA with gemini surfactants is a prerequisite to comprehending the effect of Ca^{2+} ions on the aggregation behavior of gemini surfactants in the presence of EDTA. In the literature, the interactions of EDTA with traditional monomeric surfactants in the presence of metal ions have been widely studied. Soontravanich et al.[22] found that a mixture of amphoteric surfactant DDAO with EDTA can effectively solubilize soap scum at high pH, the solubility of which is several orders of magnitude larger than that in EDTA-free systems. Moreover, the chelation of a calcium ion with

Received: September 5, 2017
Revised: October 6, 2017
Published: October 13, 2017

DOI: 10.1021/acs.langmuir.7b03137
Langmuir 2017, 33, 12719−12728

EDTA and the solubilization of stearate anions by forming mixed micelles with DDAO were hypothesized to be responsible for the dissolution of soap scum. Salahi et al.[23] found that EDTA and sodium dodecyl sulfate (SDS) are able to clean a calcium-induced, organic-fouled reverse-osmosis membrane. EDTA removes calcium ions through a ligand-exchange reaction, and SDS significantly breaks up the binding of calcium ions with foulant and then the foulant can be more easily rinsed off of the membrane surface. In addition, in the presence of EDTA, surfactants have a greater capacity to extract heavy metals such as cadmium, lead, and zinc from contaminated soil by choosing the proper type and concentration of surfactants.[24−26] These studies have demonstrated that the performance of surfactants could be significantly improved with the assistance of EDTA in metal-ion-containing systems. However, so far, the interactions of EDTA and gemini surfactants with and without calcium ions have not yet been reported. Oda's group[27,28] previously proved that tartrate containing two carboxylate groups significantly reduces the CMC of cationic ammonium gemini surfactant 14-2-14 better than does lactate containing one carboxylate group. It can be concluded that the introduction of carboxylate salts is an effective way to tune the surface activity and aggregation behavior of ionic surfactants, and the effects depend on the number of carboxylate groups. Thus, the chemical structure of EDTA containing four carboxylate groups must favor strong electrostatic interaction with cationic surfactants and generate significant effects on the aggregation of gemini surfactants. To apply ionic gemini surfactants in hard water, the effects of EDTA on the aggregation behavior of ionic gemini surfactants and the influences of calcium ions on the mixtures must be investigated in detail.

Therefore, the present work has investigated the effects of EDTA on the aggregation behavior of cationic ammonium gemini surfactant 12-6-12 and the effects of calcium ions on the EDTA/12-6-12 mixtures. The chemical structures of 12-6-12 and EDTA are presented in Scheme 1. The results demonstrate

Scheme 1. Chemical Structures of 12-6-12 and EDTA

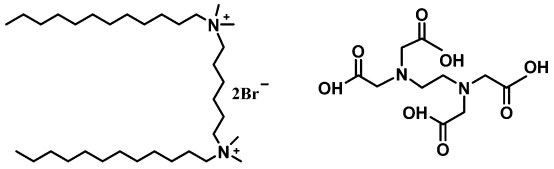

12-6-12 EDTA

that 12-6-12 and EDTA form the EDTA(12-6-12)$_2$ complex through electrostatic interaction, and the complexes undergo transitions from large network-like premicellar aggregates to small micelles with the increase in concentration. With the addition of $CaBr_2$, owing to the chelating ability to calcium ions, EDTA is partially dissociated from the complex, acting as linkages between calcium ions and surfactant molecules, and the Ca^{2+}/EDTA/12-6-12 mixture form vesicles as the $CaBr_2$ concentration increases.

EXPERIMENTAL SECTION

Materials. Ethylenediaminetetraacetic acid (EDTA, ≥99.995%) was purchased from Sigma-Aldrich. Calcium bromide ($CaBr_2$), with 99.978% min purity, was purchased from Alfa Aesar. Cationic ammounium gemini surfactant hexamethylene-1,6-bis(dodecyldimethylammonium bromide) [$C_{12}H_{25}(CH_3)_2N(CH_2)_6N(CH_3)_2C_{12}H_{25}$]$Br_2$ (12-6-12) was synthesized and purified according to the literature.[29] Milli-Q water (18 MΩ· cm^{-1}) was used in all experiments.

Surface Tension Measurements. The surface tension of the EDTA/12-6-12 aqueous solutions at different molar ratios ($R_{E/G}$) was measured using the drop volume method. Each surface tension value (γ) was determined from at least five consistent measured values, and every surface tension curve was repeated at least two times. The measurement temperature was controlled to 25.00 ± 0.05 °C using a thermostat.

Isothermal Titration Microcalorimetry (ITC). A TAM 2277-201 isothermal titration microcalorimeter (Thermometric AB, Järfälla, Sweden) was used to measure the value of the critical aggregation concentration and the enthalpy change of aggregate transitions in the mixed solution. The sample cell was initially loaded with pure water, EDTA, 12-6-12, or an EDTA/12-6-12 aqueous solution. An aqueous solution of EDTA/12-6-12, EDTA, or $CaBr_2$ solution was injected consecutively into the stirred sample cell in portions of 10 μL using a 500 μL Hamilton syringe controlled by a Thermometric 612 Lund pump until the desired concentration range was covered. During the whole titration process, the system was stirred at 60 rpm with a gold propeller, and the interval between two injections was 9 min. ΔH_{obs} was obtained by integrating the peak for each injection in the plot of heat flow P against time t. All experiments were performed at 25.0 ± 0.01 °C.

Electrical Conductivity Measurements. The conductivity of the EDTA/12-6-12 mixture at different $R_{E/G}$ values was measured as a function of surfactant concentration using a JENWAY model 4320 conductivity meter. The EDTA/12-6-12 mixed solution was titrated into water gradually, and the conductivity value was recorded until the system reached equilibrium. All measurements were performed in a temperature-controlled, double-walled glass container with the circulation of water controlled at 25.0 ± 0.1 °C.

ζ-Potential Measurements. ζ-Potential characterization of the surface charge of the aggregates in the EDTA/12-6-12 mixtures with and without $CaBr_2$ was carried out with a Malvern Zetasizer Nano-ZS instrument equipped with a thermostated chamber and a 4 mW He−Ne laser (λ = 632.8 nm). Disposable capillary cells were used for the measurements. Each sample was measured three times. All experiments were performed at 25.00 ± 0.01 °C.

Dynamic Light Scattering (DLS). DLS measurements for the EDTA/12-6-12 aggregates with and without $CaBr_2$ were performed at 25.0 ± 0.1 °C by an LLS spectrometer (ALV/SP-125) with a multi-τ digital time correlator (ALV-5000). A solid-state He−Ne laser (output power of 22 mW at λ = 632.8 nm) was used as a light source. The measurements were carried out at a scattering angle of 90°. All of the freshly prepared mixed solutions were filtered through a 450 nm membrane filter and injected into a 7 mL glass bottle. The correlation function of the scattering data was analyzed via the CONTIN method to obtain the distribution of diffusion coefficients (D) of the solutes. The apparent equivalent hydrodynamic radius (R_h) was determined using the Stokes−Einstein equation $R_h = kT/6\pi\eta D$, where k is the Boltzmann constant, T is the absolute temperature, and η is the solvent viscosity.

^{1}H NMR. ^{1}H NMR measurements of the EDTA/12-6-12 mixtures with and without $CaBr_2$ were carried out on a Bruker AV400 FT-NMR spectrometer operating at 25 ± 2 °C. Deuterium oxide (99.9%) was purchased from CIL (Cambridge Isotope Laboratories) and used to prepare the stock solutions of the mixed systems. The center of the HDO signal (4.79 ppm) was used as the reference in the D_2O solutions. In the experiments, the number of scans was adjusted to achieve good signal-to-noise ratios depending on the surfactant concentration.

Cryogenic Transmission Electron Microscopy (Cryo-TEM). The EDTA/12-6-12 mixtures with and without $CaBr_2$ were embedded in a thin layer of vitreous ice on freshly carbon-coated holey TEM grids by blotting grids with filter paper. Then the samples were plunged into liquid ethane cooled by liquid nitrogen. The frozen hydrated specimens were imaged with an FEI Tecnai 20 electron microscope (LaB6) operated at 200 kV in low-dose mode (about 2000

DOI: 10.1021/acs.langmuir.7b03137
Langmuir 2017, 33, 12719−12728

e/nm^2) and a nominal magnification of 50 000. For each specimen area, the defocus was set to 1−2 μm. Images were recorded on Kodak SO163 films and then digitized by a Nikon 9000 with a scanning step of 2000 dpi corresponding to 2.54 Å/pixel.[30]

Freeze−Fracture Transmission Electron Microscopy (FF-TEM). Samples were prepared by a freeze−fracture replica technique (FF-TEM) according to standard techniques. Fracturing and replication were carried out in a high-vacuum freeze-etching system (Balzers BAF-400D). A JEM-100CXII electron microscope was used for microscopic observation at a working voltage of 100 kV.

RESULTS AND DISCUSSION

Because EDTA is a pH-sensitive compound, the interaction between EDTA and 12-6-12 will be highly dependent on pH. EDTA has six protonation constants, i.e., the pK_a values are 0.9, 1.6, 2.0, 2.67, 6.16, and 10.26 for carboxylic groups and amino groups, respectively. At pH 7.0, most EDTA molecules carry three net negative charges due to four deprotonated carboxylic groups and one protonated amino group. Thus, pH 7.0 is chosen in all of the following investigations.

Binding of EDTA with 12-6-12. To understand the association process of EDTA with 12-6-12, an ITC experiment was carried out by titrating a 15.00 mM EDTA solution into a 5.00 mM 12-6-12 solution. The observed enthalpy changes (ΔH_{obs}) versus the EDTA/12-6-12 molar ratio ($R_{E/G}$) are presented in Figure 1. The ΔH_{obs} value for the dilution of 15.00

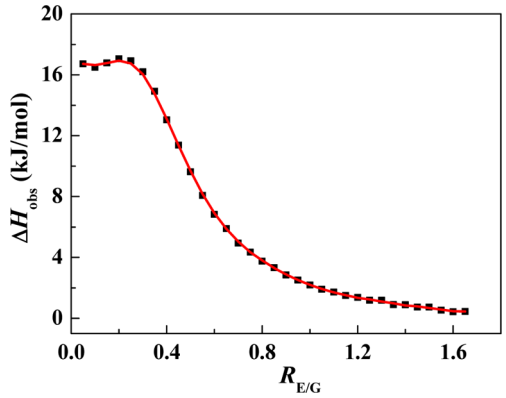

Figure 1. Variation of observed enthalpy changes (ΔH_{obs}) against the EDTA/12-6-12 molar ratio ($R_{E/G}$) by titrating 15.00 mM EDTA solution into 5.00 mM 12-6-12 solution at 25.0 °C.

mM EDTA into water has been deducted from the ITC curve. The ITC curve has a sigmoidal shape, and the value of ΔH_{obs} changes gradually from endothermic to zero. The binding number (n) of EDTA per 12-6-12 molecule is obtained by fitting the ITC curves using the standard Marquardt method with an ITC package (supplied by Microcal Inc.) embedded in an Origin program. The n value that is derived is close to 0.5, confirming the binding of EDTA with 12-6-12 in a 1:2 ratio. Because the four carboxylic groups of EDTA are deprotonated at pH 7.0, two 12-6-12 molecules are needed to saturate the binding sites of each EDTA molecule, and then the EDTA(12-6-12)$_2$ complexes are formed through intermolecular electrostatic binding in aqueous solution. Previously, our group has fabricated some oligomeric-like surfactants by using 12-6-12 and connecting molecules through noncovalent bonds.[31−33] It was found that 12-6-12 and a pH-sensitive *N*-benzoylglutamic acid (H_2Bzglu) form linear oligomeric surfactants by electrostatic attraction, $\pi-\pi$ interaction, and hydrogen bonds, and the oligomeric structures make the system efficient in forming a coacervate.[31] Tetrameric and hexameric oligomeric surfactant analogues were also formed by pH-sensitive connecting molecule (2*R*,2′*R*)-*N*,*N*′-(dodecane-1,12-diyl)bis(2,6-diaminohexanamide) (Lys-12-Lys) and SDS through electrostatic attraction and hydrogen bonding.[33] These constructed oligomeric surfactants show superior physicochemical properties without cumbersome organic synthesis and complicated purification. A recent review has summarized the progress in constructing gemini and oligomeric surfactants through noncovalent interactions.[34] Herein, that EDTA and 12-6-12 form complexes at a molar ratio of 1:2 provides another instance of constructing oligomeirc surfactants through noncovalent bonds.

EDTA and 12-6-12 molecules bind with each other in two possible ways (Figure 2): (a) each 12-6-12 molecule binds with

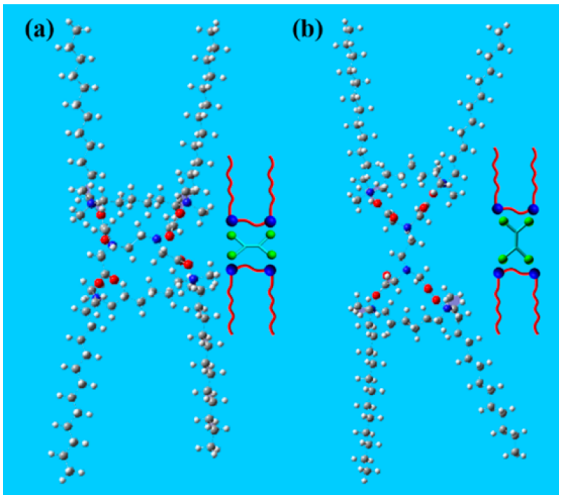

Figure 2. Two binding modes between EDTA and 12-6-12.

two carboxylate groups connected to different amino groups of EDTA or (b) each 12-6-12 molecule binds with two carboxylate groups connected to the same amino group of EDTA. The density functional theory (DFT) calculation was utilized to understand the binding mode of EDTA and 12-6-12 by the Gaussian 09 program.[35] The initial geometries of EDTA and 12-6-12 molecules were first optimized by molecular mechanics. Then, optimization calculations (a) and (b) were performed with the DFT method at the B3LYP/6-31G(d) level,[36] and the solvent (water) effect was also added. The calculated binding energy of mode (a) is 55 kJ/mol lower than that of mode (b), indicating that mode (a) is more stable for the binding between EDTA and 12-6-12.

Critical Aggregation Concentrations of the EDTA/12-6-12 Mixture. To know the surface activity and aggregation behavior of the EDTA/12-6-12 mixture, surface tension, ITC, and electrical conductivity experiments have been carried out.

Figure 3a shows the surface tension curves of the EDTA/12-6-12 aqueous solution plotted against the 12-6-12 concentration ($C_{12\text{-}6\text{-}12}$) at different $R_{E/G}$ values. The surface tension curve of pure 12-6-12 solution is also included for comparison. All surface tension curves exhibit similar varying tendencies. Upon increasing $C_{12\text{-}6\text{-}12}$, the surface tension decreases rapidly at lower concentration, and then the decrease becomes moderate beyond an inflection point. The inflection points correspond to the critical aggregation concentrations, and they are 0.58, 0.31, and 0.23 mM for $R_{E/G}$ values of 0.25, 0.50, and 1.00, respectively. These critical aggregation concentrations of the

DOI: 10.1021/acs.langmuir.7b03137
Langmuir 2017, 33, 12719−12728

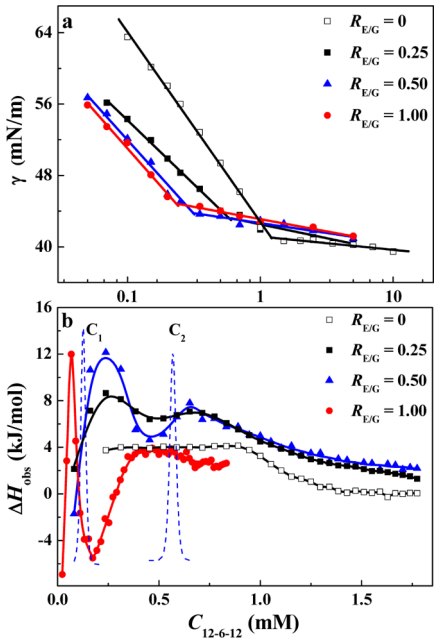

Figure 3. (a) Surface tension curves of the mixed EDTA/12-6-12 solutions plotted against the concentration of 12-6-12 ($C_{12\text{-}6\text{-}12}$) at different molar ratios ($R_{E/G}$). (b) Observed enthalpy changes (ΔH_{obs}) against $C_{12\text{-}6\text{-}12}$ by titrating EDTA/12-6-12 solution into water at $C_{12\text{-}6\text{-}12}$ = 5.00 mM for $R_{E/G}$ = 0, 0.25, and 0.50 and at $C_{12\text{-}6\text{-}12}$ = 3.00 mM for $R_{E/G}$ = 1.00. The dashed lines in (b) are the differential curves of the ITC curves for the determination of C_1 and C_2 at $R_{E/G}$ = 0.50. The temperature is 25.0 °C.

EDTA/12-6-12 mixture are lower than the CMC of pure 12-6-12, demonstrating that the EDTA/12-6-12 binding effectively screens the electrostatic repulsion between the headgroups of 12-6-12, and thus the EDTA(12-6-12)$_2$ complexes exhibit much stronger aggregation ability than the 12-6-12 molecules themselves in bulk solution. However, the corresponding γ values at the break points increase slightly with the increase in $R_{E/G}$, which may be caused by the adsorption of EDTA(12-6-12)$_2$ complexes at the air/solution interface and the resulting less tight packing of the alkyl chains of 12-6-12 at the interface limited by the steric hindrance due to the existence of EDTA. The lower aggregation concentration values and the continual decrease of γ values above the aggregation concentrations resemble the situation of tetrameric cationic surfactant PATC.[37]

Figure 3b shows the variation in ΔH_{obs} against the final surfactant concentration, whereas the EDTA/12-6-12 mixed solutions at different $R_{E/G}$ values are separately titrated into water. The ITC curve of 12-6-12 being titrated into water only has one transition point corresponding to the CMC of 12-6-12 ($R_{E/G}$ = 0); however, the ITC curves by titrating the EDTA(12-6-12)$_2$ complexes show a complicated enthalpy change process. All of the ITC curves experience a similar interaction process at different molar ratios: the ΔH_{obs} values first increases rapidly to an endothermic value and then follow a decreasing−increasing−decreasing mode. The ITC curves display two maxima and a minimum and finally coincide with the varying trend for titrating the 12-6-12 micelles into water. Two critical concentrations can be determined in the process. The situation at $R_{E/G}$ = 0.50 is taken as a representative to show the determination of the two critical concentrations (C_1 and C_2), which are located at the maxima in the differential curves of the ITC curves shown by the blue dashed lines in Figure 3b. The break points move to lower surfactant concentrations as $R_{E/G}$ increases.

To confirm the critical concentrations determined from the ITC curves, the electrical conductivity measurements were also conducted. Figure 4 shows the specific conductivity κ of the

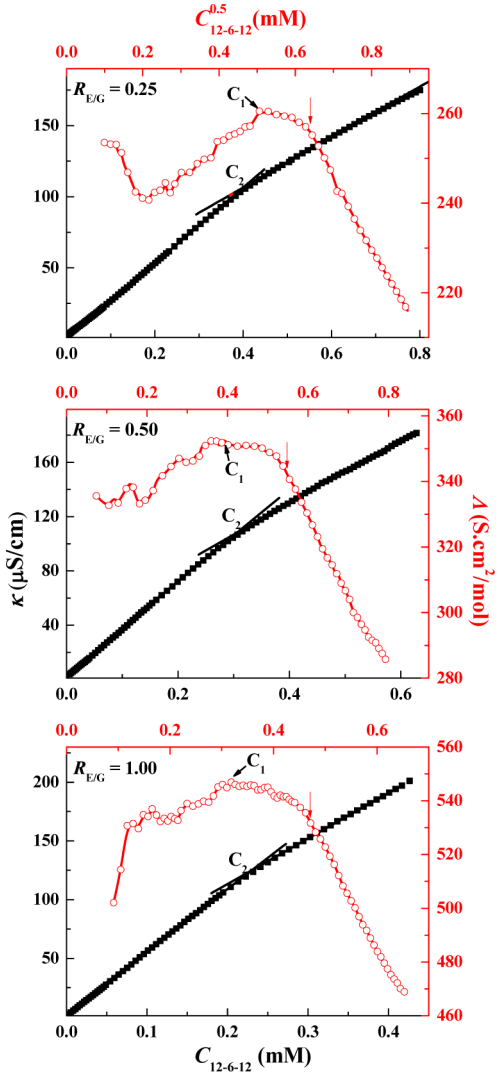

Figure 4. Variations of specific conductivity κ against the $C_{12\text{-}6\text{-}12}$ (black cube, bottom abscissa) and the molar conductivity Λ with $C^{0.5}_{12\text{-}6\text{-}12}$ (red circle, top abscissa) for the mixed solutions at different $R_{E/G}$ values and 25.0 °C.

EDTA/12-6-12 mixture against $C_{12\text{-}6\text{-}12}$ and the molar conductivity Λ against $C^{0.5}_{12\text{-}6\text{-}12}$ at different $R_{E/G}$ values, where $\Lambda = (\kappa - \kappa_0)/C_{12\text{-}6\text{-}12}$, and κ_0 is the specific conductivity of water. The appearance of the maximum in Λ against the $C^{0.5}_{12\text{-}6\text{-}12}$ curves confirms the existence of premicellar aggregates in the mixture, similar to the phenomena reported in many ionic surfactant systems.[38−40] $C_{12\text{-}6\text{-}12}$ at the Λ maximum corresponds to C_1. However, the κ values keep increasing with the increase in $C_{12\text{-}6\text{-}12}$ over the whole concentration range, but the increasing slopes decrease above a critical concentration (marked as the red arrows where Λ starts to decrease in each $\Lambda \sim C^{0.5}_{12\text{-}6\text{-}12}$ curve), the values of which are consistent with the C_2 values from the ITC curves and the critical aggregation concentrations from the surface tension curves. The critical points are normally

DOI: 10.1021/acs.langmuir.7b03137
Langmuir 2017, 33, 12719−12728

caused by the formation of micelles and the accompanying binding of counterions.

Combining all of the above results, two critical aggregation concentrations, i.e., C_1 and C_2, are determined from the clear break points of surface tension, ITC, and electrical conductivity curves at different molar ratios as summarized in Table 1. At

Table 1. Critical Aggregation Concentrations of EDTA/12-6-12 in Aqueous Solutions at Different Molar Ratios ($R_{E/G}$) Determined by Three Methods at 25.0 °C

		critical aggregation concentrations (mM)		
$R_{E/G}$		surface tension	calorimetry	conductivity
0.25	C_1		0.20	0.26
	C_2	0.58	0.59	0.40
0.50	C_1		0.14	0.13
	C_2	0.31	0.57	0.30
1.00	C_1		0.05	0.10
	C_2	0.23	0.23	0.22

mixing $R_{E/G}$ values of 0.25, 0.50, and 1.00, two critical points are found in the ITC and conductivity curves, whereas only one break point is found in the surface tension curve. The first critical points C_1 are not found in the surface tension curves, probably because the concentrations are too low and the values of the surface tension at C_1 are close to that of pure water. The second critical concentrations C_2 obtained by ITC and electrical conductivity curves are consistent with those from the surface tension curves within experimental error. Compared to the CMC value of 12-6-12 itself, the EDTA/12-6-12 mixtures show much smaller aggregation concentrations and all of the critical concentrations decrease with the increase in $R_{E/G}$, possibly because the number of oligomeric-like EDTA(12-6-12)$_2$ complexes with a stronger aggregation ability increases with the increase in $R_{E/G}$. To gain further insight into the transition process divided by C_1 and C_2, DLS, ζ-potential, and cryo-TEM measurements are carried out by taking the EDTA/12-6-12 mixture at $R_{E/G}$ = 0.50 as a representative in the following text.

Aggregate Transitions of the EDTA/12-6-12 Mixture. Figure 5a,b summarizes the distribution of the hydrodynamic radius (R_h) and zeta potential (ζ) of the EDTA/12-6-12 aggregates against $C_{12\text{-}6\text{-}12}$ at $R_{E/G}$ = 0.50. The corresponding scattering intensity from DLS measurements is shown in Figure S1. The cryo-TEM image of the EDTA/12-6-12 aggregates at a concentration beyond C_2 is shown in Figure 5c.

It is surprising that even below C_1 the EDTA/12-6-12 aggregate presents a larger size and a narrower size distribution at ~150 nm. The ζ potential of the aggregates is positive and becomes more positive with increasing concentration (Figure 5a,b). This can be attributed to the fact that the added EDTA molecules electrostatically bind with 12-6-12 and result in more compact packing of the 12-6-12 molecules with increasing concentration. Moreover, the scattering intensity of the aggregates is larger (Figure S1). Meanwhile, the initial addition of the EDTA/12-6-12 mixture generates a larger exothermic ΔH_{obs} value for a higher EDTA/12-6-12 molar ratio, suggesting that the increase in the relative content of the EDTA(12-6-12)$_2$ complexes at higher $R_{E/G}$ values leads to a larger dilution of exothermic enthalpy values. The formation of the larger aggregates may result from the joint effect of electrostatic interaction, hydrophobic interaction, and the release of counterions and dehydration of the headgroups as indicated

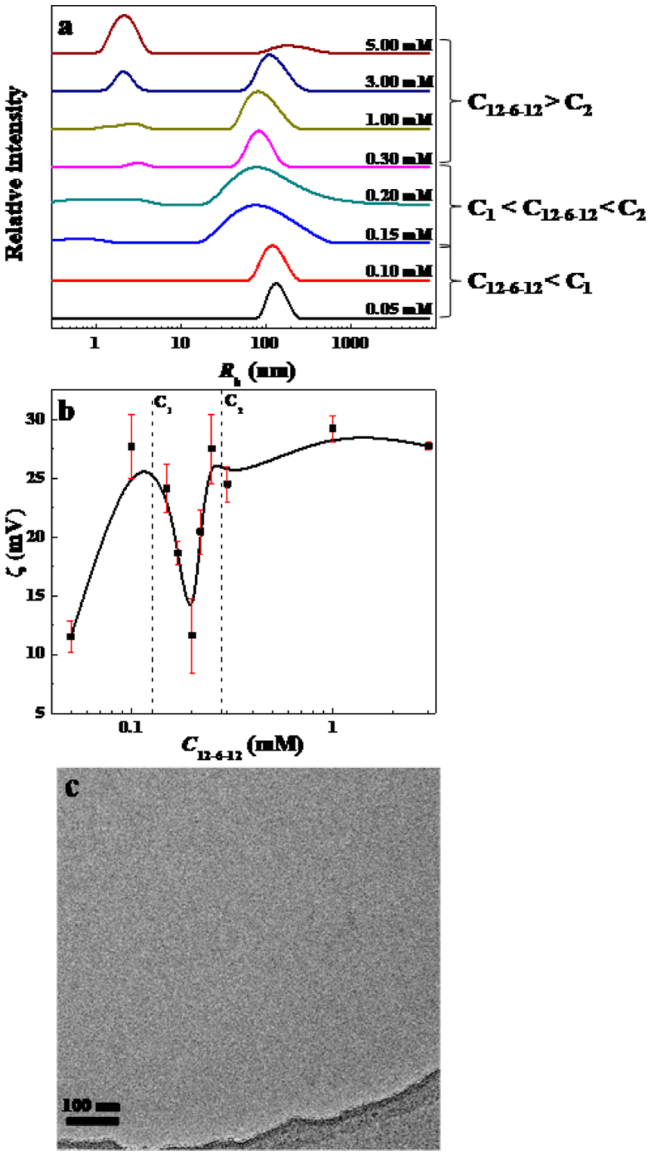

Figure 5. Distribution of hydrodynamic radius R_h (a) and zeta potential ζ (b) of the EDTA/12-6-12 aggregates against $C_{12\text{-}6\text{-}12}$ at a fixed $R_{E/G}$ of 0.50 at 25 °C. (c) Cryo-TEM image of the EDTA/12-6-12 aggregates for $C_{12\text{-}6\text{-}12}$ = 5.00 mM and C_{EDTA} = 2.50 mM.

by an increasing endothermic ΔH_{obs} in Figure 2b. The large premicellar aggregates are speculated to exhibit network structures as PATC does in the low-concentration region.[37] However, unfortunately we did not obtain clear structures of the aggregates during this period under cryo-TEM because the surfactant concentration is very low and the molecular packing may not be compact enough to be imaged.

When $C_{12\text{-}6\text{-}12}$ exceeds C_1, the scattering intensity from DLS becomes extremely weak (Figure S1) and the size distribution of the aggregate becomes very wide (Figure 5a). This means that the aggregates undergo an aggregate transition. At the same time, the ζ-potential values and ΔH_{obs} vary in a similar mode in this concentration range: fall to a minimum and then rise back to a certain value. The minimum in ζ potential and ITC curves may be attributed to the fact that the aggregate transition is accompanied by the binding of Br^- onto the headgroups of 12-6-12 in the complexes, as approved by the obvious decrease in Λ (Figure 4b).

DOI: 10.1021/acs.langmuir.7b03137
Langmuir 2017, 33, 12719−12728

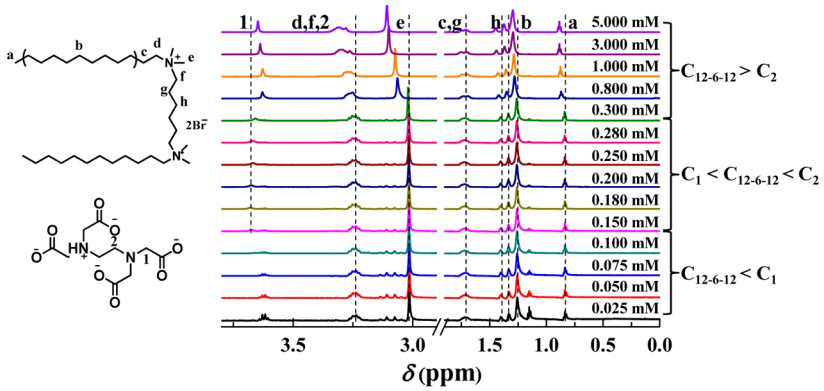

Figure 6. ^{1}H NMR spectra of the EDTA/12-6-12 aggregates against different $C_{12\text{-}6\text{-}12}$ (indicated in the plot) at a fixed $R_{E/G}$ of 0.50 and at 25 °C.

When $C_{12\text{-}6\text{-}12}$ is just above C_2, the wider size distribution around 100 nm gets narrower, and a weak distribution at ∼3 nm appears (Figure 5a). The cryo-TEM image (Figure 5c) confirms that the smaller aggregates are small micelles. As $C_{12\text{-}6\text{-}12}$ increases, the relative intensity of the larger size distribution decreases while the relative intensity of the smaller aggregates increases, and the large aggregates finally disappear. This phenomenon suggests that the large aggregates have transferred into micelles gradually. The ζ potential of micelles remains at a large positive value in this concentration range, and the ΔH_{obs} value rises to a maximum at first and then falls back to zero, showing a typical feature of the surfactant micellization process. In brief, the EDTA(12-6-12)$_2$ complexes form large premicellar aggregates below C_1, and the large aggregates transfer to micelles beyond C_2, similar to the aggregation behavior of synthesized star-shaped oligomeric surfactants that form network-like aggregates or vesicles first and then transit into micelles at high concentration.[37,41,42]

To further understand the aggregation process of the EDTA/12-6-12 mixture, a ^{1}H NMR experiment was performed. The chemical shifts of the EDTA/12-6-12 mixtures with the increase in $C_{12\text{-}6\text{-}12}$ at $R_{E/G}$ = 0.50 are shown in Figure 6. Because of the fast exchange with deuterium, the protons of the ammonium groups of EDTA show no signals in the spectra. Below C_1, the proton signals of EDTA cannot be detected because the concentration of EDTA is too low and the formation of large aggregates limits the sensitivity of the ^{1}H NMR technique. Meanwhile, the protons of 12-6-12 have no obvious shifts in this concentration range, which confirms the formation of loose aggregates before C_1. When $C_{12\text{-}6\text{-}12}$ is located between C_1 and C_2, the protons H_1 adjacent to the carboxyl groups of EDTA move upfield slowly, indicating that the spacer group of the EDTA(12-6-12)$_2$ complexes senses a more polar environment as it curves toward the bulk phase. Moreover, the binding of Br^- to the EDTA(12-6-12)$_2$ complexes also increases the shielding effect and leads to the upfield shift of proton signals. Below C_2, none of the chemical shifts of the 12-6-12 protons show any changes and the signals of H_d and H_f connected to the ammonium headgroups overlap with that of H_2 of EDTA. Beyond C_2, the chemical shifts of H_d, H_e, and H_f in the headgroup and H_a and H_b in the hydrophobic tail and the H_1 proton of EDTA move downfield to a great extent, and the signals of the H_d and H_f protons of 12-6-12 become separated from the H_2 of EDTA, indicating that the large aggregates have transferred into the small micelles and the surfactant molecules pack more tightly in the micelles with the increase in hydrophobic interaction.

Aggregate Transitions Induced by Calcium(II) Ions. Because EDTA is a chelating molecule, the transition-metal ion is expected to alter the aggregation behavior of EDTA/12-6-12 mixtures through a coordination interaction. The calcium ion was selected as a representative metal ion as frequently encountered in hard water. To eliminate the impacts of the counterions, calcium bromide ($CaBr_2$) was used in the following experiments.

ITC experiments were performed to get the binding number of calcium ions with EDTA itself and the EDTA/12-6-12 mixture ($R_{E/G}$ = 0.50). Figure 7 shows the ITC curves of the observed enthalpy (ΔH_{obs}) against the molar ratio of calcium ions to EDTA ($R_{Ca/E}$) for 5.00 mM $CaBr_2$ solution being titrated into H_2O, 5.00 mM 12-6-12, 2.50 mM EDTA, and a mixed solution of 2.50 mM EDTA and 5.00 mM 12-6-12 at 25.0 °C.

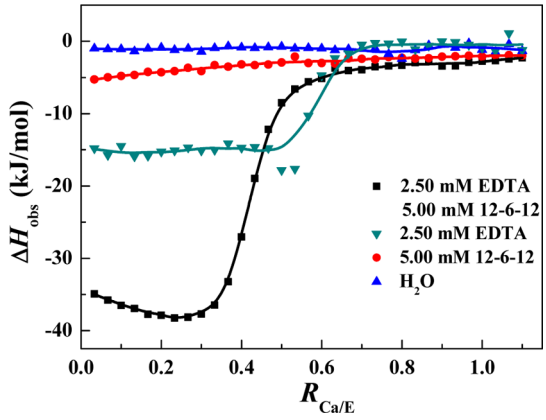

Figure 7. ITC curves of the observed enthalpy (ΔH_{obs}) against the molar ratio of calcium ions to EDTA ($R_{Ca/E}$) for 5.00 mM $CaBr_2$ solution being titrated into H_2O, 5.00 mM 12-6-12, 2.50 mM EDTA, and a mixed solution of 2.50 mM EDTA and 5.00 mM 12-6-12 at 25.0 °C.

observed enthalpy (ΔH_{obs}) against the molar ratio of calcium ions to EDTA ($R_{Ca/E}$) for 5.00 mM $CaBr_2$ solution being titrated into 2.50 mM EDTA or a mixed solution of 2.50 mM EDTA and 5.00 mM 12-6-12, respectively. For comparison, the curves of 5.00 mM $CaBr_2$ being titrated into 5.00 mM 12-6-12 and water are also presented in Figure 7. Obviously, for both the EDTA molecule and EDTA/12-6-12 mixture, the ITC curves present a similar varying tendency: ΔH_{obs} initially has large exothermic values and decreases abruptly until reaching zero, implying that the interaction is saturated finally. For the case of EDTA/12-6-12, the exothermic ΔH_{obs} value is larger than that of EDTA, suggesting a stronger coordination interaction of the calcium ion with the EDTA/12-6-12 aggregates than with pure EDTA. The ITC curve of $CaBr_2$/12-6-12 displays a very small exothermic value, so the

DOI: 10.1021/acs.langmuir.7b03137
Langmuir 2017, 33, 12719−12728

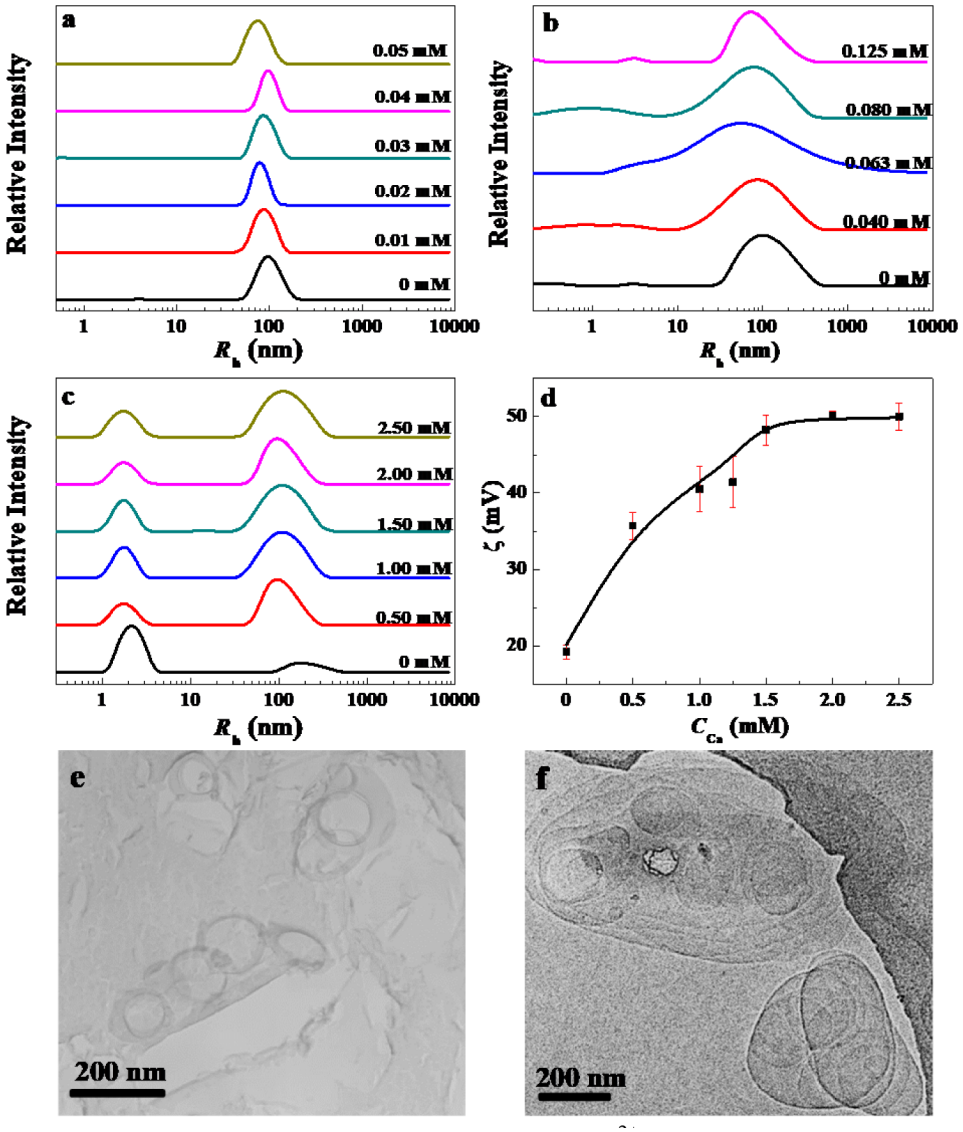

Figure 8. Distribution of hydrodynamic radius R_h of Ca^{2+}/EDTA/12-6-12 mixtures by adding different concentrations of $CaBr_2$ to a mixed solution of EDTA/12-6-12 at $R_{E/G}$ = 0.50: (a) $C_{12\text{-}6\text{-}12}$ = 0.10 mM, (b) $C_{12\text{-}6\text{-}12}$ = 0.25 mM, and (c) $C_{12\text{-}6\text{-}12}$ = 5.00 mM. For (c), the corresponding zeta potential ζ is shown in (d). (e) FF-TEM image of the Ca^{2+}/EDTA/12-6-12 aggregates for $C_{12\text{-}6\text{-}12}$ = 0.10 mM, C_{EDTA} = 0.05 mM, and C_{Ca}= 0.05 mM. (f) Cryo-TEM image of the Ca^{2+}/EDTA/12-6-12 aggregates for $C_{12\text{-}6\text{-}12}$ = 5.00 mM, C_{EDTA} = 2.50 mM, and C_{Ca} = 2.50 mM.

interaction between the calcium ion and 12-6-12 can be neglected. The binding number of Ca^{2+} obtained from the ITC curves is 0.5 for either the EDTA/12-6-12 aggregates or EDTA molecules, which means that each Ca^{2+} can bind with two EDTA molecules either in aggregates or in the molecular state. Normally, each calcium ion can complex with one EDTA molecule stoichiometrically.[43] The discrepancy with the literature may be caused by the difference in experimental conditions. Here, the pH of EDTA solution is adjusted to 7.0 by adding NaOH solution rather than phosphate-buffered solution.

To understand the influence of $CaBr_2$ on the aggregation behavior of EDTA/12-6-12, DLS experiments are performed as a function of the calcium ion concentration. In the following experiments, the EDTA/12-6-12 mixtures with 0.10, 0.25, and 5.00 mM 12-6-12 and at $R_{E/G}$ = 0.50 were selected as representatives of the three concentration regions divided by critical concentrations C_1 and C_2.

When $C_{12\text{-}6\text{-}12}$ is 0.10 mM (below C_1), the DLS results in Figure 8a show that the aggregates of Ca^{2+}/EDTA/12-6-12 exhibit one distribution at about 100 nm as the concentration of calcium ions (C_{Ca}) increases to 0.05 mM. The size distribution and the relative intensity are constant with and without $CaBr_2$. However, the EDTA/12-6-12 aggregates become vesicles with the addition of $CaBr_2$ as clearly verified by the FF-TEM image in Figure 8e. This may be attributed to the fact that the calcium ion can effectively associate with loose, large aggregates and result in more compact packing of the 12-6-12 molecules and the formation of vesicles.

When $C_{12\text{-}6\text{-}12}$ is 0.25 mM (between C_1 and C_2), Figure 8b shows that in the aggregate transition region the addition of calcium ions almost does not affect the EDTA/12-6-12 aggregates even until 0.125 mM $CaBr_2$. The aggregates maintain a very wide size distribution from 2 to 1000 nm, and the light scattering intensity of the aggregates is still relatively weak. This means that the EDTA/12-6-12 aggregates exist in the transition stage in the presence of calcium ions.

DOI: 10.1021/acs.langmuir.7b03137
Langmuir 2017, 33, 12719−12728

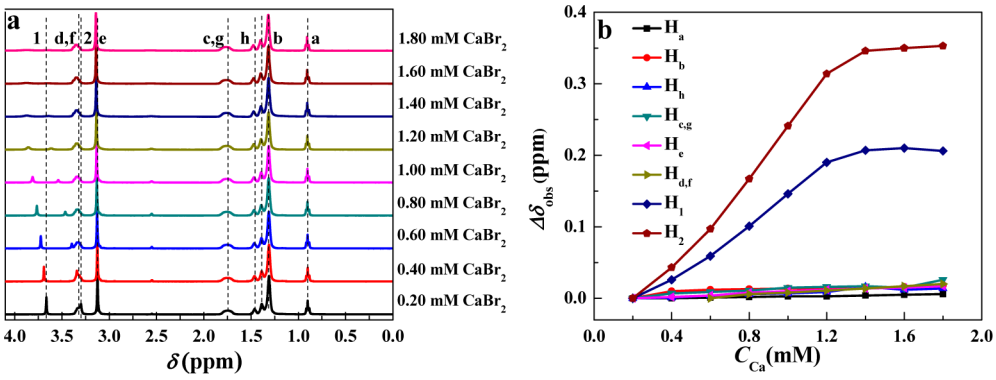

Figure 9. ^{1}H NMR spectra (a) and $\Delta\delta_{obs}$ (b) of Ca^{2+}/EDTA/12-6-12 mixtures by adding different concentrations of $CaBr_2$ (C_{Ca}) at $R_{E/G}$ = 0.50 and $C_{12\text{-}6\text{-}12}$ = 5.00 mM.

When $C_{12\text{-}6\text{-}12}$ is 5.00 mM (beyond C_2), Figure 8c indicates that the Ca^{2+}/EDTA/12-6-12 mixture presents a micelle distribution of around 2 nm and a large size distribution of around 100 nm accompanied by an increase in the scattering intensity (Figure S2). Figure 8d shows that the ζ potential of the aggregates increases gradually as C_{Ca} increases until 1.50 mM and then remains at 49 ± 3 mV. The cryo-TEM image of the mixture at C_{Ca} = 2.50 mM (Figure 8f) shows that the mixture forms vesicles with a size distribution from 50 to 250 nm, and vesicle fusion can be seen. In other words, when C_{Ca} is below 1.50 mM, calcium ions are bound on the aggregates by complexing with the carboxylate groups of EDTA, resulting in an increase in the surface charge density of aggregates. However, the calcium ions are saturated on the surface of aggregates when C_{Ca} is above 1.50 mM, and thus the size and ζ potential do not change anymore. The vesicles carry a larger number of net positive charges than the spherical micelles without calcium ions. These results imply that the addition of calcium ions induces the EDTA/12-6-12 micelles to change into vesicles in this concentration region, and the fusion of vesicles results in the formation of larger vesicles. The coordination interaction, electrostatic interaction, hydrophobic interaction, and aggregate transition from small spherical micelles to large vesicles in the Ca^{2+}/EDTA/12-6-12 mixture lead to a larger exothermic enthalpy (Figure 6).

Figure 9a shows the ^{1}H NMR spectra of Ca^{2+}/EDTA/12-6-12 mixtures by adding different concentrations of $CaBr_2$ at $R_{E/G}$ = 0.50 and $C_{12\text{-}6\text{-}12}$ = 5.00 mM and the corresponding ^{1}H NMR signal assignments. The variations in chemical shifts ($\Delta\delta_{obs}$) for the protons of 12-6-12 and EDTA against the $CaBr_2$ concentration are presented in Figure 9b for clear observation. It can be observed that all of the protons in the 12-6-12 molecule move downfield slightly as C_{Ca} increases, suggesting that the protons experience a slightly less polar microenvironment in vesicles compared to that in micelles. In particular, the chemical shifts of the H_1 and H_2 protons of the EDTA molecule shift downfield greatly and then remain at a constant value when C_{Ca} is above 1.50 mM. This means that the coordination of calcium ions with EDTA results in an electron-withdrawing effect on the carbon atoms adjacent to the carboxylate groups and ammonium groups and reduces the shielding effect on the EDTA protons. Given that each calcium ion is coordinated by two EDTA molecules, excess calcium ions cannot further change the environment of the aggregates, and thus a platform is formed in the $\Delta\delta_{obs} \sim C_{Ca}$ curve at a larger calcium ion concentration. Combined with the aforementioned ITC results, it is speculated that the coordinating interaction between the calcium ion and EDTA may lead to the partial dissociation of EDTA from the EDTA(12-6-12)$_2$ complexes, so two EDTA(12-6-12)$_2$ complexes are associated through one calcium ion. Previously, Song et al.[44] also utilized the coordination interaction to adjust the aggregate structures in the mixtures of tetradecyldimethylamine oxide and calcium oleate. The present observations indicate that chelating molecule EDTA plays a decisive role as a bridge to associate 12-6-12 and calcium ions through electrostatic binding and coordination interaction in the transition process, which in turn promotes the formation of vesicles with more compact molecular packing assisted by the hydrophobic interaction between the hydrocarbon chains of the 12-6-12 molecules.

Possible Molecular Packing. Considering all of the results and analysis above, the possible model of EDTA/12-6-12 aggregates and the aggregation transitions with the addition of calcium ions are proposed in Figure 10.

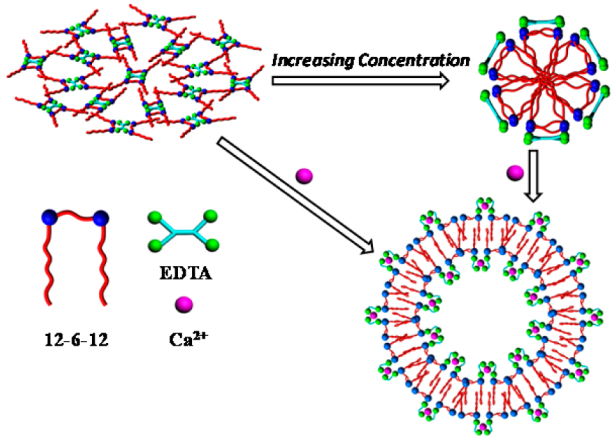

Figure 10. Proposed schematic illustrations of the variation of the aggregate morphologies in the EDTA/12-6-12 mixed solutions ($R_{E/G}$ = 0.50) with the increase in $C_{12\text{-}6\text{-}12}$ and the aggregate transitions induced by the addition of Ca^{2+}.

In the absence of calcium ions, the EDTA/12-6-12 mixture forms larger aggregates and then transfers to small micelles with the increase in the concentration, where each EDTA molecule bind to two 12-6-12 molecules through electrostatic interaction and forms oligomeric-like complex EDTA(12-6-12)$_2$. When $C_{12\text{-}6\text{-}12}$ is below C_1, large premicellar aggregates with a hydrodynamic radius of about 100 nm are formed. The

DOI: 10.1021/acs.langmuir.7b03137
Langmuir 2017, 33, 12719−12728

hydrophobic interactions among the four hydrocarbon chains of the EDTA(12-6-12)$_2$ complexes promote the entanglement of the surfactant hydrophobic tails, and the network-like aggregates may be formed in this region. As $C_{12\text{-}6\text{-}12}$ increases, the hydrophobic interaction becomes strong and the complexes pack tightly, thus small micelles are formed when $C_{12\text{-}6\text{-}12}$ reaches C_2. Previously, our group[45] and Piculell's group[46] reported that only small micelles were formed in an aqueous solution of single-chain cationic ammonium surfactant and dicarboxylate salts, whereas phase separation took place in the mixture of a single-chain surfactant with trivalent or tetravalent counterions owing to the stronger interaction of polycharged headgroups. Therefore, the gemini surfactant with tetravalent carboxylate salt EDTA shows a complicated aggregate transition compared to single-chained surfactants.

Upon the addition of calcium ions, the EDTA/12-6-12 aggregates transfer into vesicles no matter whether the original EDTA/12-6-12 aggregates are large network-like or small micelles. Because of the high affinity with EDTA, the calcium ions can occupy some binding sites of EDTA and cause the partial dissociation of EDTA from 12-6-12. Each calcium ion can interact with two EDTA(12-6-12)$_2$ complexes through a coordinating interaction with the EDTA molecules. EDTA acts as linkages between calcium ions and 12-6-12 molecules. The coordination interaction between EDTA and the calcium ion, the electrostatic interaction between EDTA and 12-6-12, and the hydrophobic interaction between the hydrocarbon chains of 12-6-12 molecules lead to an increase in the molecular packing density, resulting in the transformation of large network-like aggregates and micelles into vesicles.

CONCLUSIONS

This work investigated the aggregation behavior of cationic ammonium gemini surfactant 12-6-12 with widely used metal chelator EDTA and the effects of $CaBr_2$ on the aggregate transitions of the EDTA/12-6-12 mixtures. It is confirmed that EDTA and 12-6-12 form oligomeric surfactant analogues in a molar ratio of 1:2, and the EDTA(12-6-12)$_2$ complexes show much lower critical aggregation concentrations than 12-6-12. The complexes form large network-like premicellar aggregates at low concentrations and then transform into small micelles of ~3 nm as the concentration increases. As the molar ratio of EDTA to 12-6-12 increases from 0.25 to 1.00, the self-assembly of EDTA/12-6-12 mixtures follows the same pattern, but the critical aggregation concentrations move to smaller values. Furthermore, the addition of calcium ions affects the morphology and structure of the EDTA/12-6-12 mixture and causes either the large network-like aggregates or small micelles to change to vesicles. The results indicate that as a bridging molecule between calcium ions and the gemini surfactant the chelating molecule greatly promotes the assembly of the gemini surfactant and strengthens the aggregate packing in the presence of calcium ions. The combination of electrostatic interactions, coordination interactions, and hydrophobic interactions provides possibilities for tuning the aggregation behaviors of surfactant/chelator mixtures. This work is helpful in understanding the interaction between surfactants and chelators, provides a new way to construct oligmeric-like surfactants, and may guide the applications of this kind of gemini surfactant systems in hard water.

ASSOCIATED CONTENT

Supporting Information

The Supporting Information is available free of charge on the ACS Publications website at DOI: 10.1021/acs.langmuir.7b03137.

Scattering intensity of EDTA/12-6-12 and $CaBr_2$/EDTA/12-6-12 mixtures (PDF)

AUTHOR INFORMATION

Corresponding Author

*E-mail: yilinwang@iccas.ac.cn.

ORCID

Zhang Liu: 0000-0001-8433-6289

Yilin Wang: 0000-0002-8455-390X

Notes

The authors declare no competing financial interest.

ACKNOWLEDGMENTS

This work was supported by the National Natural Science Foundation of China (21633002) and Beijing National Laboratory for Molecular Sciences (BNLMS).

REFERENCES

(1) Mukerjee, P.; Chan, C. C. Effects of High Salt Concentrations on the Micellization of Octyl Glucoside: Salting-Out of Monomers and Electrolyte Effects on the Micelle-Water Interfacial Tension. *Langmuir* **2002**, *18*, 5375−5381.

(2) Long, F. A.; McDevit, W. F. Activity Coefficients of Non-electrolyte Solutes in Aqueous Salt Solutions. *Chem. Rev.* **1952**, *51*, 119−169.

(3) Wattebled, L.; Laschewsky, A. Effects of Organic Salt Additives on the Behavior of Dimeric ("Gemini") Surfactants in Aqueous Solution. *Langmuir* **2007**, *23*, 10044−10052.

(4) Grover, P. K.; Ryall, R. L. Critical Appraisal of Salting-Out and Its Implications for Chemical and Biological Sciences. *Chem. Rev.* **2005**, *105*, 1−10.

(5) Zapf, A.; Beck, R.; Platz, G.; Hoffmann, H. Calcium Surfactants: A Review. *Adv. Colloid Interface Sci.* **2003**, *100−102*, 349−380.

(6) Peacock, J. M.; Matijević, E. Precipitation of Alkylbenzene Sulfonates with Metal Ions. *J. Colloid Interface Sci.* **1980**, *77*, 548−554.

(7) Baviere, M.; Bazin, B.; Aude, R. Calcium Effect on the Solubility of Sodium Dodecyl Sulfate in Sodium Chloride Solutions. *J. Colloid Interface Sci.* **1983**, *92*, 580−583.

(8) Miller, D. J. Binding of Calcium Ions to Micelles-A Metallochromic Indicator Study. *Colloid Polym. Sci.* **1989**, *267*, 929−934.

(9) Stellner, K. L.; Scamehorn, J. F. Hardness Tolerance of Anionic Surfactant Solutions. 1. Anionic Surfactant with Added Monovalent Electrolyte. *Langmuir* **1989**, *5*, 70−77.

(10) Matheson, K. L.; Cox, M. F.; Smith, D. L. Interactions Between Linear Alkylbenzene Sulfonates and Water Hardness Ions. I. Effect of Calcium Ion on Surfactant Solubility and Implications for Detergency Performance. *J. Am. Oil Chem. Soc.* **1985**, *62*, 1391−1396.

(11) Yu, D.; Wang, Y.; Zhang, J.; Tian, M.; Han, Y.; Wang, Y. L. Effects of Calcium Ions on Solubility and Aggregation Behavior of an Anionic Sulfonate Gemini Surfactant in Aqueous Solutions. *J. Colloid Interface Sci.* **2012**, *381*, 83−88.

(12) Hart, J. R. Ethylenediaminetetraacetic Acid and Related Chelating Agents. *Ullmann's Encyclopedia of Industrial Chemistry*; Wiley-VCH: Weinheim, 2005.

(13) Wolf, K.; Gilbert, P. A. EDTA-Ethylenediaminetetraacetic Acid. *The Handbook of Environmental Chemistry*; Hutzinger, O., Ed.; Springer: Berlin, 1992; Vol. 3, Part F, pp 243−259.

(14) Lanigan, R. S.; Yamarik, T. A. Final Report on the Safety Assessment of EDTA, Calcium Disodium EDTA, Diammonium EDTA, Dipotassium EDTA, Disodium EDTA, TEA-EDTA, Tetraso-

DOI: 10.1021/acs.langmuir.7b03137
Langmuir 2017, 33, 12719−12728

dium EDTA, Tripotassium EDTA, Trisodium EDTA, HEDTA, and Trisodium HEDTA. *Int. J. Toxicol.* **2002**, *21*, 95−142.
(15) Menger, F. M.; Littau, C. A. Gemini Surfactants: Synthesis and Properties. *J. Am. Chem. Soc.* **1991**, *113*, 1451−1452.
(16) Menger, F. M.; Keiper, J. S. Gemini Surfactants. *Angew. Chem., Int. Ed.* **2000**, *39*, 1906−1920.
(17) Zana, R. Dimeric and Oligomeric Surfactants. Behavior at Interfaces and in Aqueous Solution: A Review. *Adv. Colloid Interface Sci.* **2002**, *97*, 205−253.
(18) Zana, R. Dimeric (Gemini) Surfactants: Effect of the Spacer Group on the Association Behavior in Aqueous Solution. *J. Colloid Interface Sci.* **2002**, *248*, 203−220.
(19) Hait, S. K.; Moulik, S. P. Gemini Surfactants: A Distinct Class of Self-assembling Molecules. *Curr. Sci.* **2002**, *82*, 1101−1111.
(20) Song, L. D.; Rosen, M. J. Surface Properties, Micellization, and Premicellar Aggregation of Gemini Surfactants with Rigid and Flexible Spacers. *Langmuir* **1996**, *12*, 1149−1153.
(21) Han, Y.; Wang, Y. L. Aggregation Behavior of Gemini Surfactants and Their Interaction with Macromolecules in Aqueous Solution. *Phys. Chem. Chem. Phys.* **2011**, *13*, 1939−1956.
(22) Soontravanich, S.; Lopez, H. E.; Scamehorn, J. F.; Sabatini, D. A.; Scheuing, D. R. Dissolution Study of Salt of Long Chain Fatty Acids (Soap Scum) in Surfactant Solutions. Part I: Equilibrium Dissolution. *J. Surfactants Deterg.* **2010**, *13*, 367−372.
(23) Salahi, A.; Gheshlaghi, A.; Mohammadi, T.; Madaeni, S. S. Experimental Performance Evaluation of Polymeric Membranes for Treatment of an Industrial Oily Wastewater. *Desalination* **2010**, *262*, 235−242.
(24) Chen, Y.; Xiong, Z.; Dong, S. Chemical Behavior of Cadmium in Purple Soil as Affected by Surfactants and EDTA. *Pedosphere* **2006**, *16*, 91−99.
(25) Doong, R.; Wu, Y.-W.; Lei, W.-G. Surfactant Enhanced Remediation of Cadmium Contaminated Soils. *Water Sci. Technol.* **1998**, *37*, 65−71.
(26) Ramamurthy, A. S.; Vo, D.; Li, X. J.; Qu, J. Surfactant-Enhanced Removal of Cu (II) and Zn (II) from a Contaminated Sandy Soil. *Water, Air, Soil Pollut.* **2008**, *190*, 197−207.
(27) Manet, S.; Karpichev, Y.; Bassani, D.; Kiagus-Ahmad, R.; Oda, R. Counteranion Effect on Micellization of Cationic Gemini Surfactants 14-2-14: Hofmeister and Other Counterions. *Langmuir* **2010**, *26*, 10645−10656.
(28) Oda, R.; Huc, I.; Schmutz, M.; Candau, S. J.; MacKintosh, F. C. Tuning Bilayer Twist Using Chiral Counterions. *Nature* **1999**, *399*, 566−569.
(29) Zana, R.; Benrraou, M.; Rueff, R. Alkanediyl-α,ω-Bis-(dimethylalky1ammonium Bromide) Surfactants. 1. Effect of the Spacer Chain Length on the Critical Micelle Concentration and Micelle Ionization Degree. *Langmuir* **1991**, *7*, 1072−1075.
(30) Hu, Z.; Tian, X.; Zhai, Y.; Xu, W.; Zheng, D.; Sun, F. Cryo-electron Microscopy Reconstructions of Two Types of Wild Rabbit Hemorrhagic Disease Viruses Characterized the Structural Features of Lagovirus. *Protein Cell* **2010**, *1*, 48−58.
(31) Wang, M.; Fan, Y.; Han, Y.; Nie, Z.; Wang, Y. L. Coacervation of Cationic Gemini Surfactant with N-Benzoylglutamic Acid in Aqueous Solution. *Langmuir* **2013**, *29*, 14839−14847.
(32) Wang, M.; Wu, C.; Tang, Y.; Fan, Y.; Han, Y.; Wang, Y. L. Interactions of Cationic Trimeric, Gemini and Monomeric Surfactants with Trianionic Curcumin in Aqueous Solution. *Soft Matter* **2014**, *10*, 3432−3440.
(33) Zhu, L.; Han, Y.; Tian, M.; Wang, Y. L. Complex Formation and Aggregate Transitions of Sodium Dodecyl Sulfate with an Oligomeric Connecting Molecule in Aqueous Solution. *Langmuir* **2013**, *29*, 12084−12092.
(34) Zhu, L.; Tang, Y.; Wang, Y. L. Constructing Surfactant Systems with the Characteristics of Gemini and Oligomeric Surfactants Through Noncovalent Interaction. *J. Surfactants Deterg.* **2016**, *19*, 237−247.
(35) Frisch, M. J.; Trucks, G. W.; Schlegel, H. B.; Scuseria, G. E.; Robb, M. A.; Cheeseman, J. R.; Scalmani, G.; Barone, V.; Mennucci, B.; Petersson, G. A.; Nakatsuji, H.; Caricato, M.; Li, X.; Hratchian, H. P.; Izmaylov, A. F.; Bloino, J.; Zheng, G.; Sonnenberg, J. L.; Hada, M.; Ehara, M.; Toyota, K.; Fukuda, R.; Hasegawa, J.; Ishida, M.; Nakajima, T.; Honda, Y.; Kitao, O.; Nakai, H.; Vreven, T.; Montgomery, J. A., Jr.; Peralta, P. E.; Ogliaro, F.; Bearpark, M.; Heyd, J. J.; Brothers, E.; Kudin, K. N.; Staroverov, V. N.; Kobayashi, R.; Normand, J.; Raghavachari, K.; Rendell, A.; Burant, J. C.; Iyengar, S. S.; Tomasi, J.; Cossi, M.; Rega, N.; Millam, N. J.; Klene, M.; Knox, J. E.; Cross, J. B.; Bakken, V.; Adamo, C.; Jaramillo, J.; Gomperts, R.; Stratmann, R. E.; Yazyev, O.; Austin, A. J.; Cammi, R.; Pomelli, C.; Ochterski, J. W.; Martin, R. L.; Morokuma, K.; Zakrzewski, V. G.; Voth, G. A.; Salvador, P.; Dannenberg, J. J.; Dapprich, S.; Daniels, A. D.; Farkas, Ö.; Ortiz, J. V.; Cioslowski, J.; Fox, D. J. *Gaussian 09*, revision C.01; Gaussian Inc.: Wallingford, CT, 2009.
(36) Lee, C.; Yang, W.; Parr, R. G. Development of the Colle-Salvetti Correlation-Energy Formula into a Functional of the Electron. *Phys. Rev. B: Condens. Matter Mater. Phys.* **1988**, *37*, 785−789.
(37) Hou, Y.; Han, Y.; Deng, M.; Xiang, J.; Wang, Y. L. Aggregation Behavior of a Tetrameric Cationic Surfactant in Aqueous Solution. *Langmuir* **2010**, *26*, 28−33.
(38) Zana, R. Alkanediyl-α,ω-Bis(dimethylalkylammonium Bromide) Surfactants. 10. Behavior in Aqueous Solution at Concentrations Below the Critical Micellization Concentration: An Electrical Conductivity Study. *J. Colloid Interface Sci.* **2002**, *246*, 182−190.
(39) Liu, Z.; Fan, Y.; Tian, M.; Wang, R.; Han, Y.; Wang, Y. L. Surfactant Selection Principle for Reducing Critical Micelle Concentration in Mixtures of Oppositely Charged Gemini Surfactants. *Langmuir* **2014**, *30*, 7968−7976.
(40) Tiwari, A. K.; Sonu; Sowmiya, M.; Saha, S. K. Study on Premicellar and Micellar Aggregates of Gemini Surfactants with Hydroxyl Substituted Spacers in Aqueous Solution Using a Probe Showing TICT Fluorescence Properties. *J. Photochem. Photobiol., A* **2011**, *223*, 6−13.
(41) Wu, C.; Hou, Y.; Deng, M.; Huang, X.; Yu, D.; Xiang, J.; Liu, Y.; Li, Z.; Wang, Y. L. Molecular Conformation-Controlled Vesicle/Micelle Transition of Cationic Trimeric Surfactants in Aqueous Solution. *Langmuir* **2010**, *26*, 7922−7927.
(42) Fan, Y.; Hou, Y.; Xiang, J.; Yu, D.; Wu, C.; Tian, M.; Han, Y.; Wang, Y. L. Synthesis and Aggregation Behavior of a Hexameric Quaternary Ammonium Surfactant. *Langmuir* **2011**, *27*, 10570−10579.
(43) Christensen, T.; Gooden, D. M.; Kung, J. E.; Toone, E. J. Additivity and the Physical Basis of Multivalency Effects: A Thermodynamic Investigation of the Calcium EDTA Interaction. *J. Am. Chem. Soc.* **2003**, *125*, 7357−7366.
(44) Song, A.; Jia, X.; Teng, M.; Hao, J. Ca^{2+}- and Ba^{2+}-Ligand Coordinated Unilamellar, Multilamellar, and Oligovesicular Vesicles. *Chem. - Eur. J.* **2007**, *13*, 496−501.
(45) Tang, Y.; Wang, R.; Wang, Y. L. Constructing Gemini-Like Surfactants with Single-Chain Surfactant and Dicarboxylic Acid Sodium Salts. *J. Surfactants Deterg.* **2015**, *18*, 25−31.
(46) Norrman, J.; Piculell, L. Phase Behavior of Cetyltrimethylammonium Surfactants with Oligo Carboxylate Counterions Mixed with Water and Decanol: Attraction between Charged Planes or Spheres with Oligomeric Counterions. *J. Phys. Chem. B* **2007**, *111*, 13364−13370.

DOI: 10.1021/acs.langmuir.7b03137
Langmuir 2017, 33, 12719−12728